



Modified Graph-Based Algorithm for Efficient Hyperspectral Feature Extraction

Asma Fejjari¹✉, Karim Saheb Ettabaa², and Ouajdi Korbaa¹

¹ MARS (Modeling of Automated Reasoning Systems) Research Laboratory.
ISITCom, University of Sousse, Sousse, Tunisia
asmafejjari@gmail.com,

Ouajdi.Korbaa@centraliens-lille.org

² IMT Atlantique, Iiti Department, Telecom Bretagne, Brest, France
karim.sahebettabaa@riadi.rnu.tn

Abstract. Since the Laplacian Eigenmaps (LE) algorithm suffers from a spectral uncertainty problem for the adjacency weighted matrix construction, it may not be adequate for the hyperspectral dimension reduction (DR), classification or detection process. Moreover, only local neighboring data point's properties are conserved in the LE method. To resolve these limitations, an improved feature extraction technique called modified Laplacian Eigenmaps (MLE) for hyperspectral images is suggested in this paper. The proposed approach determines the similarity between pixel and endmember for the purpose of building a more precise weighted matrix. Then, based on the obtained weighted matrix, the DR data are derived as the Laplacian eigenvectors of the Laplacian matrix, constructed from the weighted matrix. Furthermore, the novel proposed approach focuses on maximizing the distance between no nearby neighboring points, which raises the separability among ground objects. Compared to the original LE method, experiment results, for hyperspectral images classification and detection tasks, have proved an enhanced accuracy.

Keywords: Laplacian eigenmaps · Hyperspectral dimension reduction
Endmember extraction · Hyperspectral images

1 Introduction

Hyperspectral images (HSI) [1], picked up from remote sensing airborne satellites, provide a very detailed information about the collected scenes; which results a various level of challenge during data processing. Practically, dimension reduction is a fundamental issue of the HSI high dimension problem. While keeping the important data properties, the dimension reduction concept is aimed to get a set of points $Y = \{\mathbf{y}_1, \mathbf{y}_2, \dots, \mathbf{y}_l\}$ in \mathbb{R}^d , from the original data set $X = \{\mathbf{x}_1, \mathbf{x}_2, \dots, \mathbf{x}_l\} \in \mathbb{R}^n$ where $d \ll n$. Therefore, a great set of dimension reduction techniques has been proposed in the last decade. These techniques can be categorized into two main branches: global methods, such like Isometric Mapping (ISOMAP) and Diffusion Maps (DM), and local methods as Locally Linear Embedding (LLE) and Laplacian Eigenmaps (LE) [2, 3].

The global approaches seek to keep the global data properties, while local approaches aim to preserve the local criteria of the manifold.

In this paper, our main focus is to improve the existing Laplacian Eigenmaps (LE) technique [3]. In fact, LE is a local dimension reduction method where the original data is constructed from a graph. The construction of the low dimensional space is achieved by minimizing the distance between data points and its neighbors. Consequently, the choice of the distance metric, used during adjacency graph construction, is an essential element due to its direct impact on the performance of dimensionality reduction. Euclidean distance, employed by the original LE algorithm, is susceptible to variations in the spectrum magnitudes, which can be generated by different factors such as illuminations, atmospheric changes, and sensor noise [11]. Subsequently, the selection of the neighbor pixels based on the Euclidean distance generates errors during the adjacency graph construction.

In this paper, we propose spectral angle based LE method that uses the similarity between pixels and endmembers [10] instead of the Euclidian distance, measures the similarity between two pixels. Additionally, this attempt serves to increase the separability between the different classes of the scene by maximizing the distance between non-nearest neighboring points.

The rest of this paper is organized as follows: The next section presents the LE algorithm, followed by a detailed description of the MLE method. Section 4 describes the experiment process and results followed by conclusions and future works.

2 Laplacian Eigenmaps (LE)

LE [3] is a well-known local feature extraction technique which is based on the spectral graph theory. Using Laplacian graph concept, the LE technique builds a dataset neighborhood graph and computes a transformation matrix that maps data points to the low dimension subspace. The LE algorithm includes three main steps:

1. Constructing a weighted graph G : G is built by looking for the k nearest neighbors of each point, using the Euclidian distance metric.
2. Defining the weighted matrix: Based on the graph G , weights may be computed as follows:

$$\omega_{ij} = \begin{cases} e^{-\frac{\|x_i - x_j\|^2}{\sigma}}, & \text{if } i \text{ and } j \text{ are connected} \\ 0 & , \text{ otherwise} \end{cases} \quad (1)$$

σ is a defined spectral scale parameter.

3. Deriving the Laplacian eigenvalues and eigenvectors: LE tends to preserve the local data properties, in the low-dimensional subspace, by optimizing the following objective function:

$$\arg \min \sum_{ij} \|y_i - y_j\|^2 \omega_{ij} \quad (2)$$

Eigenvalues and eigenvectors, describing the dimension reduction data, can be obtained from the following generalized eigenvector problem:

$$\mathbf{Y}\mathbf{L} = \lambda\mathbf{Y}\mathbf{D} \quad (3)$$

\mathbf{D} is a diagonal weighted matrix where $D_{i,i} = \sum_j \omega_{i,j}$, $\mathbf{L} = \mathbf{D} - \boldsymbol{\omega}$ represents the Laplacian matrix and λ accords to the d -smallest nonzero eigenvalues of (3).

3 Proposed Approach

The LE algorithm attempts to minimize the distance between data points and its neighbors, adopting the Euclidian distance. However, for hyperspectral images, LE often fails. This is caused by changes in spectrum magnitudes, particularly for a data points from small size classes [11]. To address this issue, we proposed a new approach, called modified LE (MLE), to construct an adjacency graph in which, for a given data point \mathbf{x}_i , its nearest neighbors appertained to the same ground object of \mathbf{x}_i while others do not. In the MLE, a spectral-based distance, derived from the similarity between pixel and endmember [10], is used to define the neighbors of each data point. Furthermore, the proposed MLE interested more in widening the distances among the non-closest neighbors. The MLE algorithm can be summarized as follows:

1. Extract endmember spectra from hyperspectral image using the vertex component analysis (VCA) method [8]; then, based on the spectral angle distance, the similarity between pixel spectra and the endmember spectra can be computed. Extracted endmembers can be represented as a matrix $\mathbf{M} = (\mathbf{m}_1, \mathbf{m}_2, \dots, \mathbf{m}_E)$, where $\mathbf{m}_i (i = 1, 2, \dots, E)$ is a $n \times 1$ vector that represents the i^{th} endmember, n is the spectral bands' number and E is the endmembers' number.
2. Build the adjacency graph: Adopting the spectral angle distance metric can more indeed reduce the error produced by the spectral amplitude variations. The spectral angle distance, between each pixel and endmember, can be computed as bellow:

$$D_j^i = d(\mathbf{m}_i, x_j) = \arccos \left[\frac{\sum_{k=1}^n \frac{m_{ik} - x_{jk}}{(\sum_{k=1}^n m_{ik}^2)^{1/2} (\sum_{k=1}^n x_{jk}^2)^{1/2}}}{\sum_{k=1}^n \frac{m_{ik} - x_{jk}}{(\sum_{k=1}^n m_{ik}^2)^{1/2} (\sum_{k=1}^n x_{jk}^2)^{1/2}}} \right] \quad (4)$$

The k nearest neighbors of each pixel can be selected, referred to (5):

$$d'(x_i, x_j) = \sum_k \left| \left(\frac{D_i^k - D_{\min}^k}{D_{\max}^k - D_{\min}^k} \right) - \left(\frac{D_j^k - D_{\min}^k}{D_{\max}^k - D_{\min}^k} \right) \right| \quad (5)$$

Hence, we can construct an adjacency graph G' and calculate the adjacency weighted matrix $\boldsymbol{\omega}'$ based on (6) and (7).

$$G'_{ij} = \begin{cases} 1 & , \text{ if } x_i \text{ and } x_j \text{ are nearest neighbors} \\ 0 & , \text{ otherwise} \end{cases} \quad (6)$$

$$\omega'_{ij} = \begin{cases} e^{-d'(\mathbf{x}_i, \mathbf{x}_j)\sigma^2}, & \text{if } \mathbf{x}_j \in N(\mathbf{x}_i) \\ 0, & \text{otherwise} \end{cases} \quad (7)$$

While D'_j represents the spectral angle distance between the j^{th} pixel and i^{th} end-member, D^k_{\min} and D^k_{\max} show the minimum and maximum distances between all pixels and the k^{th} endmember, respectively, and $N(\mathbf{x}_i)$ determines the k nearest neighbor set of (\mathbf{x}_i) .

3. Solve the optimization problem: The novel Laplacian Eigenmaps (MLE) technique tends to project data point from the original space to the low-dimensional space in such a way that, the distances between nearest neighbors is reserved, i.e., local properties and the distances between non-neighboring points is maximized. This is reflected to optimize the following objective function:

$$\arg \max \sum_{ij} \|\mathbf{y}_i - \mathbf{y}_j\|^2 \omega'_{ij} \quad (8)$$

Maximum eigenvalues and eigenvectors are calculated from the next eigendecomposition problem:

$$\mathbf{Y}\mathbf{L}' = \lambda\mathbf{Y}\mathbf{D}' \quad (9)$$

\mathbf{D}' represents the diagonal weighted matrix, defined by $D'_{ii} = \sum_j \omega'_{ij}$, $\mathbf{L}' = \mathbf{D}' - \omega'$ corresponds to the Laplacian matrix and $\{\lambda_i\}_{i=1}^d$ conforms to the d -smallest eigenvalues of (9).

4 Experiment Process and Results

This section is dedicated to examine the suggested method efficiency. The modified LE approach was assessed during hyperspectral images classification and detection tasks; then compared according to the original LE accuracy results. The architecture of the suggested technique is shown in Fig. 1.

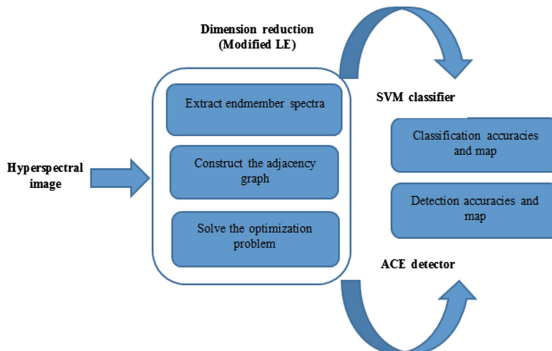


Fig. 1. The flowchart of the proposed approach.

4.1 Classification Tasks

For the classification tasks, the Indian Pines hyperspectral data set, collected in the north of Indiana (United States of America) in 1992 by the Airborne Visible/Infrared Imaging Spectrometer (AVIRIS) sensor system, was adopted. The used scene covers 204 spectral bands of size 145×145 pixels, in the spectral range 0.4–2.5 μm ; it includes 16 classes as shown in Fig. 2. The Indian Pines image and its reference map were downloaded from [4]. As the SVM (Support Vector Machine) classifier [5] was performed to classify test data set, only 10% of each class pixels, picked randomly, were implemented as the input training samples. Each classification script was iterated ten times and the mean of the classification accuracies was used to judge classification performance. Overall accuracy (OA), average accuracy (AA) and kappa coefficient [9] were used to assess the proposed technique yield. We took $k = 20$, $n = 20$ and $\sigma = 1$ for the LE technique and the proposed feature extraction method. Table 1 summarizes classification results of the proposed MLE and the original LE technique, and Fig. 3 gives their classification maps. The best overall accuracy (OA) was obtained from the MLE approach as it provided 79,60%, while the kappa coefficient was 77,20%. The OA of original LE was 68,92% and the kappa coefficient was 65,17%. The proposed technique is characterized by its capability of improving the classification accuracies of the original LE technique by about 11% of overall accuracy. To more understand the novel suggested approach, we selected samples from the four first classes, C1, C2, C3 and C4. Figure 4 represents spectral curves of the four exploited classes, in which each spectrum represents one ground object. We selected 100 samples for each class and the reduced dimensionality of the MLE was two bands (band 21 and 50).

Figure 5 displays the projected data obtained by LE and the proposed approach. The results obtained by LE showed that this method is incapable of preserving the global structure of data properties. In fact, LE has a weak effect in terms of classes' separation; i.e. not all of the nearest neighbors come from the same ground object. The proposed MLE algorithm can separate widely the four selected classes.



Fig. 2. Pseudo-color image, ground truth map and labels of the used hyperspectral scene.

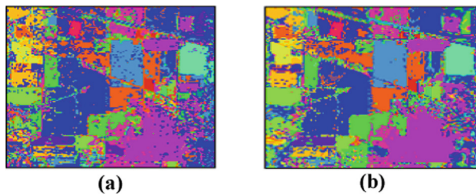


Fig. 3. Classification maps obtained by (a) the original LE and (b) the proposed approach.

Table 1. Classification results obtained by the LE and the MLE techniques.

Classes	No. of samples	LE	MLE
C1	46	99,98	99,99
C2	1428	89,00	93,51
C3	830	94,03	95,49
C4	237	98,44	99,25
C5	483	98,83	99,47
C6	730	96,48	97,92
C7	28	99,92	99,89
C8	478	99,21	99,92
C9	20	99,48	99,79
C10	972	95,27	96,89
C11	2455	84,09	92,27
C12	593	94,82	96,40
C13	205	99,38	99,54
C14	1265	96,28	99,14
C15	386	96,39	99,14
C16	93	99,89	99,89
OA (%)		68,92	79,60
AA (%)		96,37	97,95
Kappa (%)		65,17	77,20

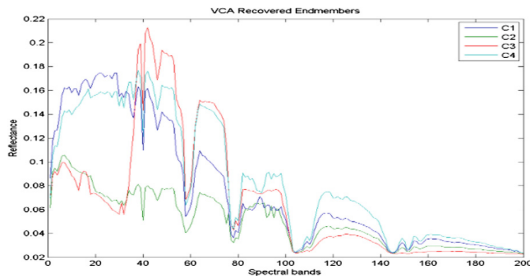


Fig. 4. Spectral curves of the first four classes in the Indian Pines data set.

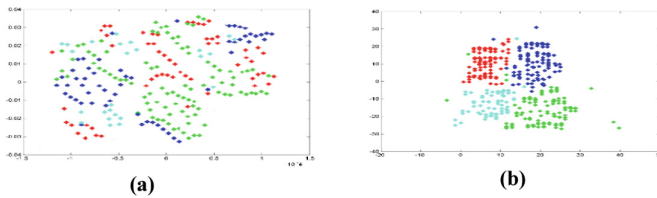


Fig. 5. Projected data produced by (a) LE and (b) MLE.

4.2 Detection Tasks

Urban-1 hyperspectral scene, selected from the Airport-Beach-Urban (ABU) hyperspectral data set, was used for target detection tasks. The adopted image contains 204 bands, each band is of size 100×100 pixels and a spatial resolution of 17,2 m per pixel. The Urban-1 scene, captured in Texas Coast in August of 2010, was collected by the AVIRIS sensor system and downloaded from [6]. Figure 6 shows the Urban-1 image and its detection map. The Adaptive Cosine/Coherence Estimator (ACE) detector [7] and the Receiver Operating Characteristic (ROC) curve metric were adopted to evaluate the qualitative results. The ROC curve is computed from probability of detection (PD) versus false alarm rate (FAR), at different values of threshold. Experimentally, $k = 200, n = 15$ and $\sigma = 1$, were chosen as optimal parameters for the MLE technique. The threshold was fixed from 0 to 255, and the ROC curves of LE and MLE techniques are presented in Fig. 7. When the false alarm rate varies from 0 to 1, the proposed method permits higher detection accuracy. In comparison with the original LE method, the proposed technique enhanced the true positive detection rate. The detection maps of the original LE and the suggested approach are shown in Fig. 8. By visualizing the two maps, we find that our proposed approach tends to be less attracted by false detection. Moreover, the MLE can detect the target objects clearly, especially the small ones.

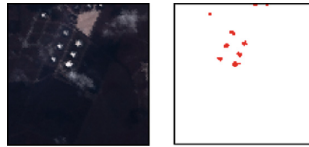


Fig. 6. Color composites of the Urban-1 hyperspectral scene and its detection map.

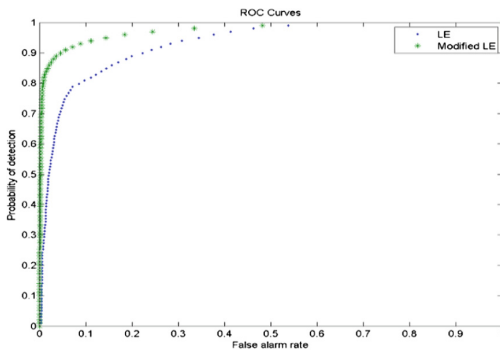


Fig. 7. ROC curves of LE and modified LE methods.

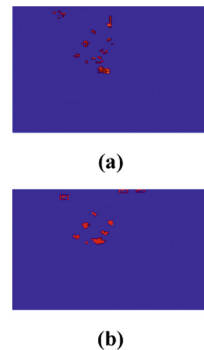


Fig. 8. Detection maps of (a) LE and (b) MLE techniques.

5 Conclusions and Future Works

This study is aimed to resolve the spectral uncertainty problem for the adjacency weighted matrix construction, for the Laplacian Eigenmaps (LE) approach. In this light, we proposed a modified version of LE, titled modified LE, for hyperspectral image classification and target detection. In a different way to the original LE, a spectral based distance derives from the similarity between pixel and endmember is used to define the neighbors of each data point. Besides to preserving local properties, the proposed approach tends to keep the global structure of original data. Experiments, during classification and detection tasks, demonstrated that MLE is characterized by a superior outstanding capacity compared to the original LE. In addition to spectral elements, spatial components are paramount to improve the MLE yield, which is seen very encouraging for future works.

Acknowledgment. This work was supported and financed by the Ministry of Higher Education and Scientific Research of Tunisia.

References

1. Camps-Valls, G., Tuia, D., Bruzzone, L., Benediktsson, J.A.: Advances in hyperspectral image classification: earth monitoring with statistical learning methods. *IEEE Signal Process. Mag.* **31**(1), 45–54 (2014)
2. Khodr, J., Younes, R.: Dimensionality reduction on hyperspectral images: a comparative review based on artificial datas. In: 2011 4th International Congress on Image and Signal Processing, pp. 1875–1883. IEEE, Shanghai, China (2011)
3. Hou, B., Zhang, X., Ye, Q., Zheng, Y.: A novel method for hyperspectral image classification based on laplacian eigenmap pixels distribution-flow. *IEEE J. Sel. Top. Appl. Earth Obs. Remote Sens.* **6**(3), 1602–1618 (2013)
4. Computational Intelligence search group site. [http://www.ehu.es/ccwintco/index.php?title = Hyperspectral_Remote_Sensing_Scenes](http://www.ehu.es/ccwintco/index.php?title=Hyperspectral_Remote_Sensing_Scenes). Last accessed 05 Dec 2017
5. Chang, C.-C., Lin, C.-J.: LIBSVM: a library for support vector machines. *ACM Trans. Intell. Syst. Technol.* **2**(3), 1–27 (2011)
6. Xudong Kang's home page. <http://xudongkang.weebly.com/data-sets.html>. Last accessed 24 Dec 2017
7. Alvey, B., Zare, A., Cook, M., Ho, D.K.C.: Adaptive coherence estimator (ACE) for explosive hazard detection using wideband electromagnetic induction (WEMI). In: SPIE Conference Detection and Sensing of Mines, Explosive Objects, and Obscured Targets XXI, Baltimore (2016)
8. Nascimento, J.M.P., Dias, J.M.B.: Vertex component analysis: a fast algorithm to unmix hyperspectral data. *IEEE Trans. Geosci. Remote Sens.* **43**(4), 898–910 (2005)
9. Fejjari, A., Saheb Ettabaï, K., Korbaï, O.: Modified schroedinger eigenmap projections algorithm for hyperspectral imagery classification. In: IEEE/ACS 14th International Conference on Computer Systems and Applications (AICCSA), pp. 809–814. IEEE, Hamammet, Tunisia (2017)

10. Wang, Y., Huang, S., Liu, Z., Wang, H., Liu, D.: Locality preserving projection based on endmember extraction for hyperspectral image dimensionality reduction and target detection. *Appl. Spectrosc.* **70**(9), 1573–1581 (2016)
11. Yan, L., Niu, X.: Spectral-angle-based laplacian eigenmaps for nonlinear dimensionality reduction of hyperspectral imagery. *Photogramm. Eng. Remote Sens.* **80**(9), 849–861 (2014)